HIPPOCAMPUS 13:801–805 (2003)

Intracellular Correlate of EPSP-Spike Potentiation in CA1 Pyramidal Neurons Is Controlled by GABAergic Modulation

Nathan P. Staff and Nelson Spruston*

Department of Neurobiology and Physiology, Institute for Neuroscience, Northwestern University, Evanston, Illinois

ABSTRACT: The hippocampus has been used extensively as a model to study plastic changes in the brain's neural circuitry. Immediately after high-frequency stimulation to hippocampal Schaffer collateral axons, a dramatic change occurs in the relationship between the presynaptic CA3 and the postsynaptic CA1 pyramidal neurons. For a fixed excitatory postsynaptic potential (EPSP), there arises an increased likelihood of action potential generation in the CA1 pyramidal neuron. This phenomenon is called EPSP-spike (E-S) potentiation. We explored E-S potentiation, using patch-clamp techniques in the hippocampal slice preparation. A specific protocol was developed to measure the action potential probability for a given synaptic strength, which allowed us to quantify the amount of E-S potentiation for a single neuron. E-S potentiation was greatest when γ-aminobutyric acid (GABA)ergic inhibition was intact, suggesting that modulation of inhibition is a major aspect of E-S potentiation. Expression of E-S potentiation also correlated with a reduced action-potential threshold, which was greatest when GABAergic inhibition was intact. Conditioning stimuli produced a smaller threshold reduction when inhibition was blocked, but some reduction also occurred in the absence of a conditioning stimulus. Together, these results suggest that E-S potentiation is caused primarily through a reduction of GABAergic inhibition, leading to larger EPSPs and reduced action potential threshold. Our findings do not rule out, however, the possibility that modulation of voltage-gated conductances also contributes to E-S potentiation.

KEY WORDS: plasticity; hippocampus; excitability; dialysis; patch-clamp recording

Bliss and Lomo (1973) reported a long-lasting change in synaptic strength from the perforant path to dentate gyrus synapse that was elicited by tetanic stimulation. In these in vivo extracellular recordings, there were two main findings: (1) the field excitatory postsynaptic potential (EPSP) increased after tetanic stimulation and persisted for ≤10 h; and (2) there was a disproportionate increase in the population spike for a given EPSP size. The first finding is the well-studied long-term potentiation (LTP) of glutamatergic synapses. The second finding is what has become known as EPSP-spike (E-S) potentiation.

Two main hypotheses have been developed to account mechanistically for the phenomenon of E-S potentiation. First, E-S potentiation could be the result of decreased inhibition within the hippocampal circuitry. In this way, after tetanic stimulation, a given excitatory synaptic current results in an increased EPSP amplitude due to the decreased inhibition, thus bringing the postsynaptic neuron closer to action potential threshold. The second hypothetical mechanism for E-S potentiation is that a post-tetanus change occurs in the intrinsic electrical properties of postsynaptic neurons. Such changes could result in enhanced propagation of EPSPs toward the action potential initiation site in the axon or a lowering of the threshold for action potential generation. These two primary theories for the mechanisms of E-S potentiation—changes in excitation-inhibition versus changes in postsynaptic electrical properties—are not mutually exclusive, but the relative importance of each continues be debated and tested in the literature. This report examines the cellular mechanisms of E-S potentiation using patch-clamp recording in the acute hippocampal slice preparation. A preliminary report of this work has appeared in abstract form (Staff and Spruston, 2001).

Transverse hippocampal slices (300 μm) were made from 5–9-week-old Wistar rats; visually guided patch-clamp recordings were made from CA1 pyramidal neurons, as described previously (Staff et al., 2000). Throughout the experiments, brain slices were bathed in oxygenated (i.e., bubbled with 95% O_2, 5% CO_2) artificial cerebrospinal fluid (ACSF), containing (in mM): 125 mM NaCl, 2.5 mM KCl, 2 mM $CaCl_2$, 1 mM $MgCl_2$, 25 mM $NaHCO_3$, 1.25 mM NaH_2PO_4, 25 mM glucose. Whole-cell current-clamp recordings were made from cells using an electrode connected to a bridge amplifier (Dagan BVC-700). Patch-clamp electrodes were pulled from glass capillary tubes and were fire polished and filled with intracellular solution containing (in mM): potassium gluconate 115, KCl 20, sodium phosphocreatinine 10, HEPES 10, MgATP 2, NaGTP 0.3, and 0.1% biocytin for subsequent determination of morphol-

Grant sponsor: National Institutes on Drug Abuse; Grant number: F30 DA14206; Grant sponsor: National Institutes of Neurological Disorders and Stroke; Grant number: R01 NS35180.
*Correspondence to: Nelson Spruston, Department of Neurobiology and Physiology, Northwestern University, 2205 Tech Drive, Evanston, IL 60208. E-mail: spruston@northwestern.edu
Accepted for publication 18 November 2002
DOI 10.1002/hipo.10129

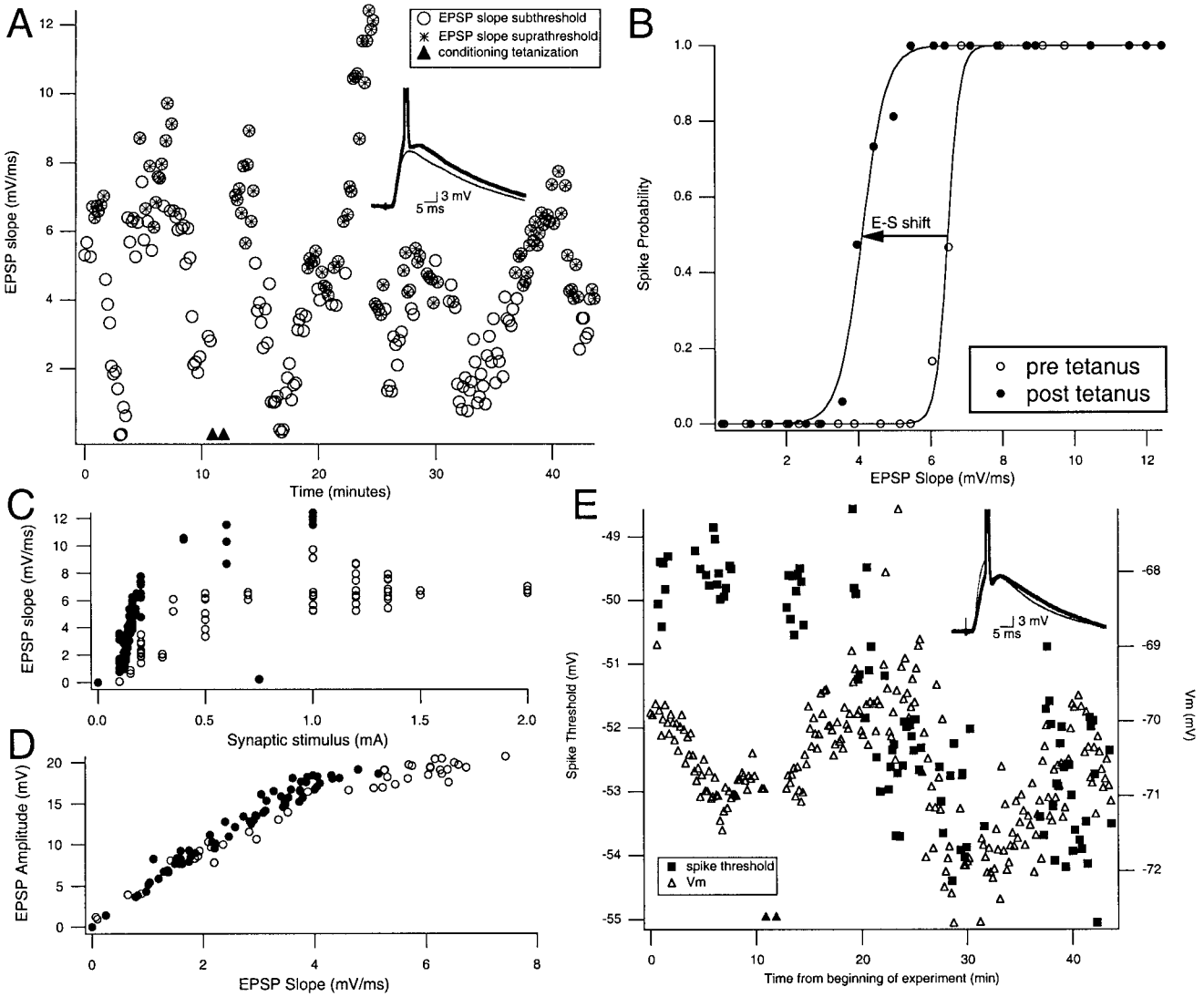

FIGURE 1. Conditioning stimulation results in an increased likelihood of action potential generation for a given excitatory postsynaptic potential (EPSP) strength. All data shown are from a single CA1 pyramidal neuron. A: By changing synaptic stimulation intensity, a range of EPSP strengths are gathered both before and after a high-frequency conditioning stimulation (a 1-s 100-Hz train delivered twice at a 1-min interval) is delivered to Schaffer collateral fibers (at 50% maximal intensity). Circles filled with asterisks indicate where an action potential occurred. Inset: Two traces with the same EPSP slope. After tetanic stimulation, the identical EPSP slope results in an action potential (thick line), whereas before it was subthreshold (thin lines). B: Construction of EPSP-spike (E-S) curves. Data from A were grouped into 0.5-mV/ms bins, and the frequency of action potential initiation was calculated, both before and after tetanic stimulation. The subsequent EPSP slope vs spike probability curves are fit with a sigmoid curve. The E-S shift is calculated as the shift between the two curves at the 0.5 spike probability point. E-S shift = 2.37 mV/ms. C: EPSP slope as a function of stimulus intensity. Note that for a given synaptic stimulus, the EPSP slope is increased after tetanization, demonstrating potentiation of the synapses. Symbols are the same as in B. D: Relationship between EPSP slope and amplitude. There is no difference before and after tetanic stimulation. Symbols are the same as in B. E: Plot of both resting membrane potential (△, V_m) and absolute threshold for action potential generation (■). Note the drop in action potential threshold after tetanic stimulation (also illustrated in inset).

ogy. Electrode resistance in the bath ranged within 2–4 MΩ, and series resistance ranged within 9–35 MΩ. Capacitance compensation and bridge balance were performed online. Cells were discarded if series resistance exceeded 35 MΩ or if the resting membrane potential changed by >3 mV during the course of an experiment. Synaptic stimulation was elicited using either a tungsten bipolar electrode or a large patch pipette filled with ACSF connected to a stimulus isolator (Axon). To prevent epileptic discharges in the slice, which commonly occur when α-aminobutyric acid (GABA)ergic inhibition is blocked, the CA3 region was microdissected out of each slice before recording. EPSP strength was estimated using a linear fit to the 15–50% amplitude range between baseline V_m and either the EPSP peak or action-potential voltage threshold. Conditioning stimuli consisted of two 1-s 100 Hz trains (repeated at 1-min intervals) or a theta-burst protocol (5 stimuli at 100 Hz delivered 25–50 times at 5 Hz).

To elicit and assess E-S potentiation, the following protocol was designed. During the first 10 min of whole-cell recording, data to determine the EPSP-spike relationship were gathered by varying the synaptic stimulation strength (delivered at 0.1 Hz), while recording the resulting EPSP slope and spike generation. After a conditioning protocol (either theta-burst or 100-Hz tetanic stimulation), the EPSP-spike relationship was determined again (Fig. 1A). The EPSP-spike data were compiled into a graph depicting the relationship between the EPSP slope and spike probability both before and after the test stimulus (Fig. 1B). To do this, data were binned into groups based on their EPSP slope (bins of 0.5 mV/ms). Within each binned group, the probability of firing an action potential was determined and fit with a sigmoid function (the E-S curve).

After the conditioning stimulus, a leftward shift was observed in the E-S curve, which was quantified as the shift of the EPSP slope corresponding to 50% spike probability. The conditioning stimulus also caused a leftward shift in the relationship between EPSP slope and stimulus intensity (Fig. 1C), which is characteristic of LTP induction. The relationship between EPSP amplitude and slope was relatively unchanged, but EPSPs triggered action potentials at EPSP slopes and amplitudes that were subthreshold before conditioning (Fig. 1D). These changes were caused by a distinct reduction in the action-potential threshold after the conditioning stimulus (Fig. 1E). This experimental design and analysis of the EPSP slope-spike probability relation and action potential threshold were used in all experiments in this study.

To determine the role of inhibition in the generation of E-S potentiation, experiments were performed in either normal ACSF (nACSF) or ACSF containing GABA-A and GABA-B receptor blockers (4 μM SR95531 and 1 μM CGP55845A, respectively). EPSP amplitude increased after application of GABA-A/B receptor antagonists, but EPSP slope was not affected (data not shown). E-S potentiation was significantly reduced when experiments were performed in the presence of GABA-receptor blockers (compared with the nACSF group), suggesting that a large portion of E-S potentiation requires intact inhibition ($P < 0.05$; Fig. 2). Although some E-S potentiation occurred in the presence of GABA blockers, the amount was not significantly different than when no high-frequency stimulation was applied in GABA blockers ($P > 0.05$).

In addition to alterations in the excitation-inhibition synaptic balance, we investigated whether there were changes in the postsynaptic intrinsic neuronal properties associated with the high-frequency synaptic conditioning stimulus. There were no significant changes in either resting potential or input resistance after the conditioning stimulus (resting potential: -66.0 ± 0.7 mV before conditioning, -66.2 ± 0.7 mV after conditioning; input resistance: 57.7 ± 2.4 MΩ before conditioning, 57.4 ± 2.4 MΩ after conditioning; $n = 21$, pooled data from different pharmacological conditions). In all neurons, however, there was an overall increased excitability that developed during the recordings, which was reflected in a decreased action-potential threshold (measured as V_m at the beginning of the steeply rising action potential) evoked either by synaptic stimulation or somatically injected current ($P < 0.05$; Fig. 3). The lowered action potential threshold was correlated with the amount of E-S potentiation that occurred ($r^2 = 0.39$, $P = 0.0001$ for synaptic stimulation, $r^2 = 0.48$, $P = 0.0005$ for current injection; simple linear regression). In some of these experiments, the lowered action potential threshold developed shortly after the conditioning stimulus was delivered, suggesting a causative role for the conditioning stimulus on the threshold (e.g., see Fig. 1D). However, the fact that nearly all neurons exhibited a threshold reduction, even when no conditioning stimulus was applied, suggests that intracellular dialysis may also reduce the action-potential threshold. The threshold reduction was slightly larger when inhibition was intact, but this difference failed to reach statistical significance (Fig. 3).

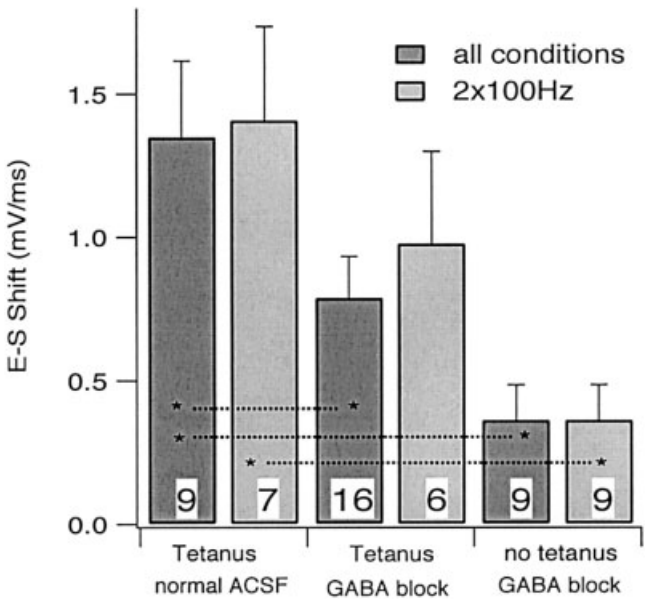

FIGURE 2. Excitatory postsynaptic potential-spike (E-S) potentiation is largest when inhibition is intact, as measured by the E-S shift. The three experimental conditions are (1) high-frequency conditioning stimulus in normal artificial cerebrospinal fluid (nACSF), (2) high-frequency conditioning stimulus in constant presence of γ-aminobutyric acid (GABA)-A/B receptor blockade, and (3) no conditioning stimulus in constant presence of GABA-A/B receptor blockade. The conditioning stimulus used was either tetanic or theta-burst (see Materials and Methods). A subset of neurons in which two 1-s 100-Hz tetanization were delivered (repeated at 1-min intervals) is also presented separately. Asterisks indicate statistical significance compared with conditioning in nACSF, where $P < 0.05$, using Tukey's multiple comparisons after one-way analysis of variance (ANOVA). The number of neurons in each condition is indicated at the bottom of each bar.

Our results provide further support for the hypothesis that altered inhibition is the primary mechanism of E-S potentiation. Previous studies with extracellular field recordings have shown that addition of picrotoxin to the bath causes a potentiation of the population spike that is disproportionately large compared with the potentiation of the population EPSP. Some researchers have shown that subsequent tetanization in picrotoxin does not change this relationship (Abraham et al., 1987; Chavez-Noriega et al., 1989), suggesting that changes in inhibition could lead to E-S potentiation. A more recent study provides strong evidence that

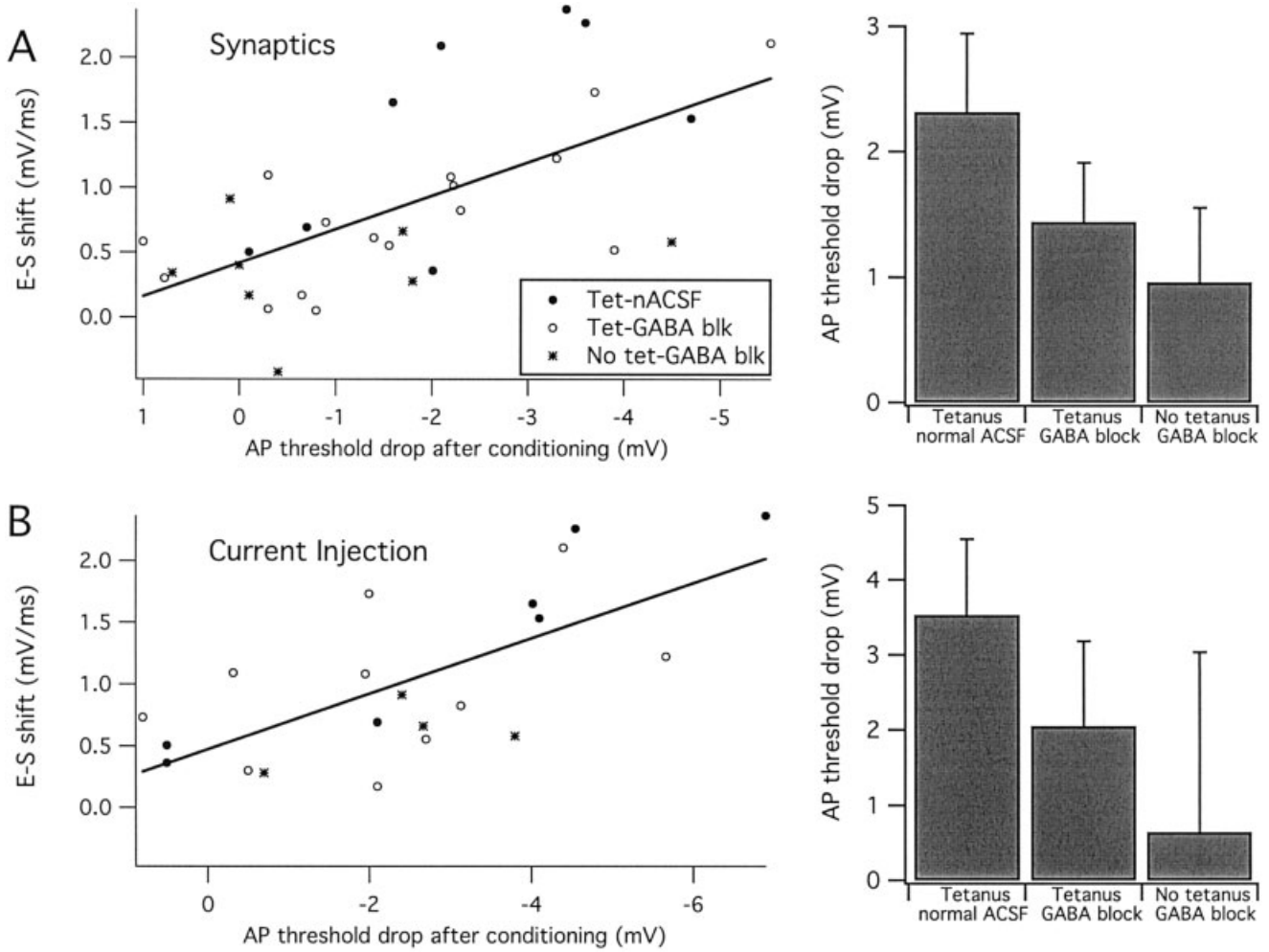

FIGURE 3. Action potential threshold changes in CA1 pyramidal neurons are correlated with the amount of excitatory postsynaptic potential (EPSP)-spike (E-S) shift. A: Correlation of action potential threshold drop with E-S shift for all neurons in all conditioning protocols, with synaptic stimulation. Summary bar graph is on the right ($P > 0.05$). B: Correlation of action potential threshold drop with E-S shift for all neurons in all conditioning protocols, with somatic current injection. Summary bar graph is on the right ($P > 0.05$).

after tetanization, in addition to the LTP of the AMPA-mediated response, there is a long-term depression of the $GABA_A$ receptor, which is NMDA-receptor dependent and is mediated by activation of calcineurin, a calcium-dependent protein phosphatase (Lu et al., 2000). Furthermore, transgenic mice that overexpress calcineurin are unable to exhibit E-S potentiation (Lu et al., 2000).

While these studies and our own research consistently point to downregulation of inhibition as an important component of E-S potentiation, the reasons for this modulation are unclear. One possibility is that GABAergic transmission may be directly decreased after tetanic stimulation; another possibility is that EPSPs onto inhibitory interneurons may be depressed after tetanic stimulation (McMahon and Kauer, 1997; McBain et al., 1999). Although other studies have demonstrated LTP of EPSPs onto inhibitory interneurons (Christie et al., 2000; Perez et al., 2001), the net effect of conditioning stimuli in our experiments must be toward LTD of excitatory drive onto interneurons and/or depression of inhibitory postsynaptic potentials (IPSPs), to produce E-S potentiation.

There is also some evidence for changes in the intrinsic excitability of the postsynaptic neuron during E-S potentiation. Some researchers have observed E-S potentiation in the presence of GABA antagonists, leading to speculation that changes of intrinsic conductances may play a role (Hess and Gustafsson, 1990; Jester et al., 1995). Studies have also indicated a decrease in the absolute voltage threshold for action potential firing after high-frequency stimulation associated with E-S potentiation (Chavez-Noriega et al., 1990; Jester et al., 1995).

The statistically significant correlation between the amount of E-S potentiation and the shift in action-potential threshold in our study strongly suggests that a reduction in action-potential threshold may contribute to E-S potentiation (Fig. 3). The fact that this shift was largest when inhibition was intact suggests that a reduction in inhibition may contribute to a lower action-potential threshold, as expected for the reduction of an outward current. Interestingly, the threshold reduction was apparent for current-evoked as well as synaptically evoked action potentials, suggesting that regulation of tonic inhibition may contribute to the threshold

shift. In contrast, a reduction of action-potential threshold was also observed when GABAergic transmission was blocked, suggesting that regulation of voltage-gated conductances might also play a role. Unfortunately, these conclusions are complicated by the fact that the action-potential threshold was reduced even when a conditioning stimulus was not applied, suggesting that cytoplasmic dialysis may affect neuronal excitability. This observation underscores the importance of careful controls when examining activity-induced changes in neuronal excitability; it also indicates that more experiments are required to elucidate the significance and mechanisms of action-potential threshold shifts in E-S potentiation.

While our study examined possible changes in action-potential threshold measured in the soma, another possible target of activity-dependent modulation is dendritic excitability. For example, current-source density analyses have demonstrated a shift of current sinks into the dendrite after high-frequency stimulation, consistent with increased dendritic electrogenesis (Taube and Schwartzkroin, 1988; Vida et al., 1995). In addition, the increased EPSPs associated with LTP and the reduced inhibition that leads to E-S potentiation are likely to increase the probability of dendritic spiking in CA1 neurons (Golding and Spruston, 1998; Golding et al., 1999). Similarly, shifts in the distribution of synaptic strength could increase dendritic excitability indirectly by activating more excitatory or fewer inhibitory synapses on individual dendritic branches. These intriguing observations suggest that repetitive synaptic activation may lead to multiple alterations of dendritic integration as a result of synaptic and nonsynaptic plasticity.

Acknowledgments

This work was supported by grant F30 DA14206 from the National Institutes on Drug Abuse (to N.P.S.) and by grant R01 NS35180 from the National Institutes of Neurological Disorders and Stroke (to N.S.).

REFERENCES

Abraham WC, Gustafsson B, Wigstrom H. 1987. Long-term potentiation involves enhanced synaptic excitation relative to synaptic inhibition in guinea-pig hippocampus. J Physiol (Lond) 394:367–380.

Bliss TV, Lomo T. 1973. Long-lasting potentiation of synaptic transmission in the dentate area of the anaesthetized rabbit following stimulation of the perforant path. J Physiol (Lond) 232:331–356.

Chavez-Noriega LE, Bliss TV, Halliwell JV. 1989. The EPSP-spike (E-S) component of long-term potentiation in the rat hippocampal slice is modulated by GABAergic but not cholinergic mechanisms. Neurosci Lett 104:58–64.

Chavez-Noriega LE, Halliwell JV, Bliss TV. 1990. A decrease in firing threshold observed after induction of the EPSP-spike (E-S) component of long-term potentiation in rat hippocampal slices. Exp Brain Res 79:633–641.

Christie BR, Franks KM, Seamans JK, Saga K, Sejnowski TJ. 2000. Synaptic plasticity in morphologically identified CA1 stratum radiatum interneurons and giant projection cells. Hippocampus 10:673–683.

Golding NL, Spruston N. 1998. Dendritic sodium spikes are variable triggers of axonal action potentials in hippocampal CA1 pyramidal neurons. Neuron 21:1189–1200.

Golding NL, Jung H, Mickus T, Spruston N. 1999. Dendritic calcium spike initiation and repolarization are controlled by distinct potassium channel subtypes in CA1 pyramidal neurons. J Neurosci 19:8789–8798.

Hess G, Gustafsson B. 1990. Changes in field excitatory postsynaptic potential shape induced by tetanization in the CA1 region of the guinea-pig hippocampal slice. Neuroscience 37:61–69.

Jester JM, Campbell LW, Sejnowski TJ. 1995. Associative EPSP-spike potentiation induced by pairing orthodromic and antidromic stimulation in rat hippocampal slices. J Physiol (Lond) 484(Pt 3):689–705.

Lu YM, Mansuy IM, Kandel ER, Roder J. 2000. Calcineurin-mediated LTD of GABAergic inhibition underlies the increased excitability of CA1 neurons associated with LTP. Neuron 26:197–205.

McBain CJ, Freund TF, Mody I. 1999. Glutamatergic synapses onto hippocampal interneurons: precision timing without lasting plasticity. Trends Neurosci 22:228–235.

McMahon LL, Kauer JA. 1997. Hippocampal interneurons express a novel form of synaptic plasticity. Neuron 18:295–305.

Perez Y, Morin F, Lacaille JC. 2001. A hebbian form of long-term potentiation dependent on mGluR1a in hippocampal inhibitory interneurons. Proc Natl Acad Sci USA 98:9401–9406.

Staff NP, Spruston N. 2001. Intracellular correlate of EPSP-spike potentiation in CA1 pyramidal neurons is controlled by GABAergic pathways. Presented at the Society for Neuroscience Meeting San Diego, CA.

Staff NP, Jung H, Thiagarajan T, Yao M, Spruston N. 2000. Resting and active properties of pyramidal neurons in subiculum and CA1 of rat hippocampus. J Neurophysiol 84:2398–2408.

Taube JS, Schwartzkroin PA. 1988. Mechanisms of long-term potentiation: a current-source density analysis. J Neurosci 8:1645–1655.

Vida I, Czopf J, Czeh G. 1995. A current-source density analysis of the long-term potentiation in the hippocampus. Brain Res 671:1–11.